Chemical Science

ROYAL SOCIETY OF CHEMISTRY

EDGE ARTICLE

View Article Online
View Journal | View Issue

Open Access Article. Published on 15 January 2021. Downloaded on 11/26/2025 5:09:30 PM.
This article is licensed under a Creative Commons Attribution-NonCommercial 3.0 Unported Licence.

Check for updates

Cite this: *Chem. Sci.*, 2021, **12**, 3599

All publication charges for this article have been paid for by the Royal Society of Chemistry

Rhodium-catalysed selective C–C bond activation and borylation of cyclopropanes†

Yandong Wang,‡ Jingyi Bai,‡ Youqing Yang,‡ Wenxuan Zhao, Yong Liang,* Di Wang, Yue Zhao and Zhuangzhi Shi*

Received 10th November 2020
Accepted 14th January 2021

DOI: 10.1039/d0sc06186g

rsc.li/chemical-science

Transition metal (TM)-catalysed directed hydroboration of aliphatic internal olefins which facilitates the construction of complex alkylboronates is an essential synthetic methodology. Here, an efficient method for the borylation of cyclopropanes involving TM-catalysed directed C–C activation has been developed. Upon exposure to neutral Rh(I)-catalyst systems, *N*-Piv-substituted cyclopropylamines (CPAs) undergo proximal-selective hydroboration with HBpin to provide valuable γ-amino boronates in one step which are otherwise difficult to synthesize by known methods. The enantioenriched substrates can deliver chiral products without erosion of the enantioselectivities. Versatile synthetic utility of the obtained γ-amino boronates is also demonstrated. Experimental and computational mechanistic studies showed the preferred pathway and the origin of this selectivity. This study will enable the further use of CPAs as valuable building blocks for the tunable generation of C–heteroatom or C–C bonds through selective C–C bond activation.

Introduction

Alkylboronic esters[1] are highly important in all facets of chemical science, ranging from synthetic chemistry[2] to materials science[3] to drug discovery.[4] Traditionally, these compounds can be prepared by the well-known Brown hydroboration, in which the *syn*-addition of hydroboranes to alkenes follows an anti-Markovnikov manner.[5] During the past decades, the TM-catalysed hydroboration of aliphatic internal olefins with tethered directing groups has shown interesting chemo-, regio-, and diastereoselectivity, which greatly complements the classical noncatalytic process (Fig. 1A).[6] The coordination of directing groups with the TM catalysts can deliver hydroboration products with controllable distal[7] and/or proximal[8] selectivity. Recently, directed borylation of aliphatic C–H bonds with proximal[9] and distal[10] selectivity has also gained momentum. The functionalization of the C–C bond is one of the most attractive strategies in organic chemistry. Despite the significant advances, transformations that allow the selective borylation of single C–C bonds remain effectively unknown.

CPAs are among the most prevalent molecules found in feedstock chemicals, drug molecules, and natural products.[11] In this context, they have been exploited as robust building blocks in organic synthesis, including C–H and C–C bond functionalizations.[12] Seminal work by Itami and Yamaguchi described the *N*-Piv-directed C–H borylation of CPAs with *cis* selectivity using phenanthroline-based ligands and a catalytic amount of an iridium salt (Fig. 1B).[13] Inspired by the success of directed borylation of alkenes and alkanes, we envisioned that the borylation of CPAs by chelation-assisted C–C bond activation[14] could provide a unique opportunity to access amino-containing boronates as potent protease inhibitors.[15] During the preparation of this paper, Yamaguchi and Yokogawa reported a related transformation achieved by C–C hydroboration of CPAs using an iridium catalyst and ^{t}Bu-Quinox as the ligand (Fig. 1C).[16] Notably, this elegant chemistry exhibited excellent distal selectivity, resulting in β-methyl alkylboronates. In contrast, herein, we describe a simple and practical method to achieve hydroboration of CPAs *via* proximal C–C bond cleavage affording γ-amino boronates in the presence of a rhodium complex and a simple phosphine ligand (Fig. 1D). A series of mechanistic experiments and DFT calculations revealed the preferred pathway of this transformation, which provides high proximal-selectivity by the slightly catalytic system.

Results and discussion

Reaction design

Examination and optimisation of the reaction parameters were explored using CPA **1a** as the substrate and pinacolborane (HBpin) as the borylating source in conjunction with various TM catalysts and ligands (Table 1). As reported,[16] when the

State Key Laboratory of Coordination Chemistry, Chemistry and Biomedicine Innovation Center (ChemBIC), School of Chemistry and Chemical Engineering, Nanjing University, Nanjing 210093, China. E-mail: shiz@nju.edu.cn; yongliang@nju.edu.cn

† Electronic supplementary information (ESI) available. CCDC 2032397–2032399. For ESI and crystallographic data in CIF or other electronic format see DOI: 10.1039/d0sc06186g

‡ These authors contributed equally to this work.

Open Access Article. Published on 15 January 2021. Downloaded on 11/26/2025 5:09:30 PM.
This article is licensed under a Creative Commons Attribution-NonCommercial 3.0 Unported Licence.

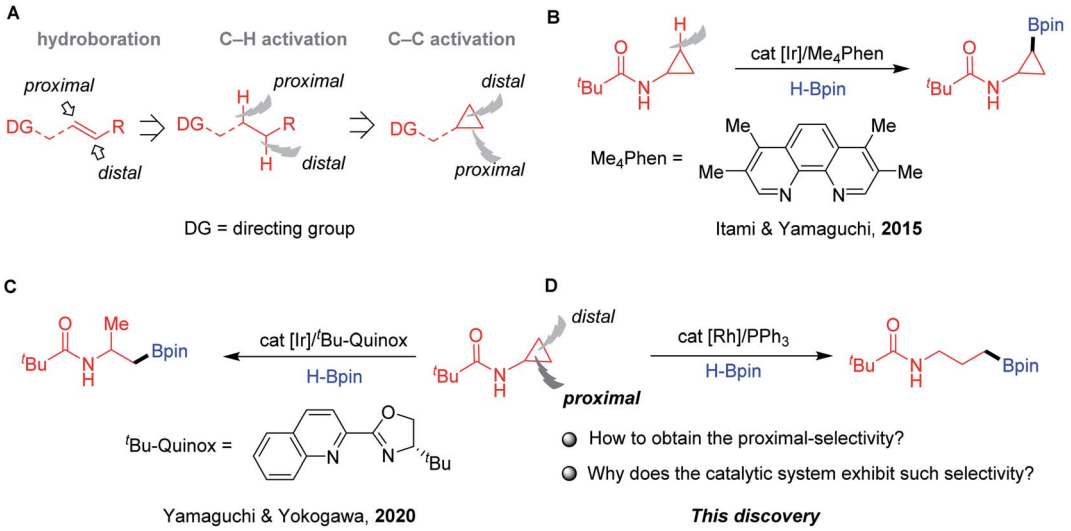

Fig. 1 TM-catalysed borylation of olefins and CPAs. (A) The development of TM-catalysed directed borylation. (B) Ir-catalysed directed C–H borylation of CPAs. (C) Ir-catalysed distal-selective hydroboration of CPAs. (D) Rh-catalysed proximal-selective hydroboration of CPAs.

Table 1 Optimisation of reaction conditions for the proximal-selective hydroboration of CPA **1a** [a]

Entry	[M] (mol%)	Ligand (mol%)	Solvent	**2a**/**3a**[b]	Yield of **2a**[b] (%)
1	$[Ir(cod)OMe]_2$ (5)	^{t}Bu-Quinox (2.5)	Toluene	5/95	Trace
2	$[Ir(cod)OMe]_2$ (1)	PPh_3 (4)	Toluene	>99/1	42
3	$[Rh(CO)_2Cl]_2$ (1)	PPh_3 (4)	Toluene	>99/1	47
4	$[Rh(coe)_2Cl]_2$ (1)	PPh_3 (4)	Toluene	>99/1	52
5	**$[Rh(cod)Cl]_2$ (1)**	**PPh_3 (4)**	**Toluene**	**>99/1**	**99 (91)**[c]
6	$Rh(PPh_3)_3Cl$ (1)	—	Toluene	>99/1	65
7	$[Rh(OAc)_2]_2$ (1)	PPh_3 (4)	Toluene	>99/1	4
8	$[Rh(cod)Cl]_2$ (1)	PPh_3 (4)	^{c}Hexane	>99/1	76
9	$[Rh(cod)Cl]_2$ (1)	PPh_3 (4)	THF	>99/1	70
10[d]	$[Rh(cod)Cl]_2$ (1)	PPh_3 (4)	Toluene	>99/1	73
11[e]	$[Rh(cod)Cl]_2$ (1)	PPh_3 (4)	Toluene	—	0
12	$[Rh(cod)Cl]_2$ (0.5)	PPh_3 (2)	Toluene	>99/1	85
13	$[Rh(cod)Cl]_2$ (1)	PPh_3 (2)	Toluene	>99/1	79
14	$[Rh(cod)Cl]_2$ (1)	—	Toluene	—	8
15	—	PPh_3 (4)	Toluene	—	0

[a] Reaction conditions: cat [M] (0.5–5 mol%), **L** (2–4 mol%), **1a** (0.20 mmol), HBpin (0.60 mmol) in solvent (1.0 mL), 24 h, 130 °C, under Ar, in sealed Schlenk tubes. [b] Determined by GC-MS analysis. [c] Yield of purified compounds after chromatography. [d] At 120 °C. [e] Using B_2pin_2 instead of HBpin.

reactions were performed with 5 mol% $[Ir(cod)OMe]_2$ as the catalyst and 2.5 mol% ^{t}Bu-Quinox as the ligand at 130 °C for 24 h in toluene, branched boronate **3a** was formed in 52% yield together with a small amount of the linear byproduct **2a** (**2a**/**3a** = 5/95, entry 1). In this study, we focused our attention on product **2a**. Completely inverse selectivity (**2a**/**3a** > 99/1) was observed with 1 mol% Ir catalyst and 4 mol% PPh_3, in which the desired product **2a** was obtained in 42% yield (entry 2). Moreover, we found that Rh(I) complexes were more effective than the Ir catalyst. Upon switching the catalyst to $[Rh(CO)_2Cl]_2$, the yield of **2a** further increased to 47% (entry 3). Other Rh(I) complexes, such as $[Rh(coe)_2Cl]_2$, provided the corresponding product **2a** in 52% yield (entry 4), and $[Rh(cod)Cl]_2$ was the most efficient, giving a 99% yield of **2a** (entry 5). When Wilkinson's

 © 2021 The Author(s). Published by the Royal Society of Chemistry

Open Access Article. Published on 15 January 2021. Downloaded on 11/26/2025 5:09:30 PM.
This article is licensed under a Creative Commons Attribution-NonCommercial 3.0 Unported Licence.

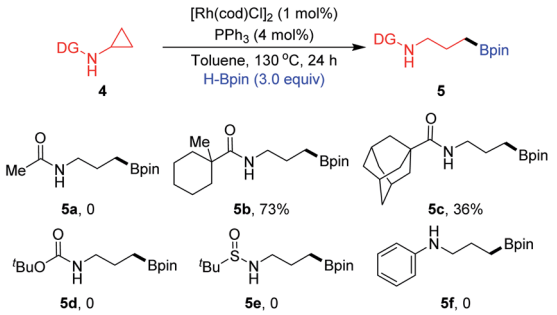

Scheme 1 Evaluating different *N*-substituents.

catalyst ($Rh(PPh_3)_3Cl$) was used instead of $[Rh(cod)Cl]_2$ and PPh_3, the reaction provided **2a** in a much lower yield (entry 6). Under these reaction conditions, upon switching to a Rh(II) catalyst, the reaction became very sluggish (entry 7). The replacement of toluene by other solvents such as ^{c}hexane and THF provided acceptable yields of **2a** (entries 8 and 9). The effect of temperature was also examined, and 120 °C was found to be less optimal (entry 10). Furthermore, the use of HBpin is crucial to this borylation process; other classes of borylating sources such as B_2pin_2 did not afford any borylation product (entry 11). Furthermore, decreasing the Rh catalyst loading to 0.5 mol%

Table 2 Substrate scope[a]

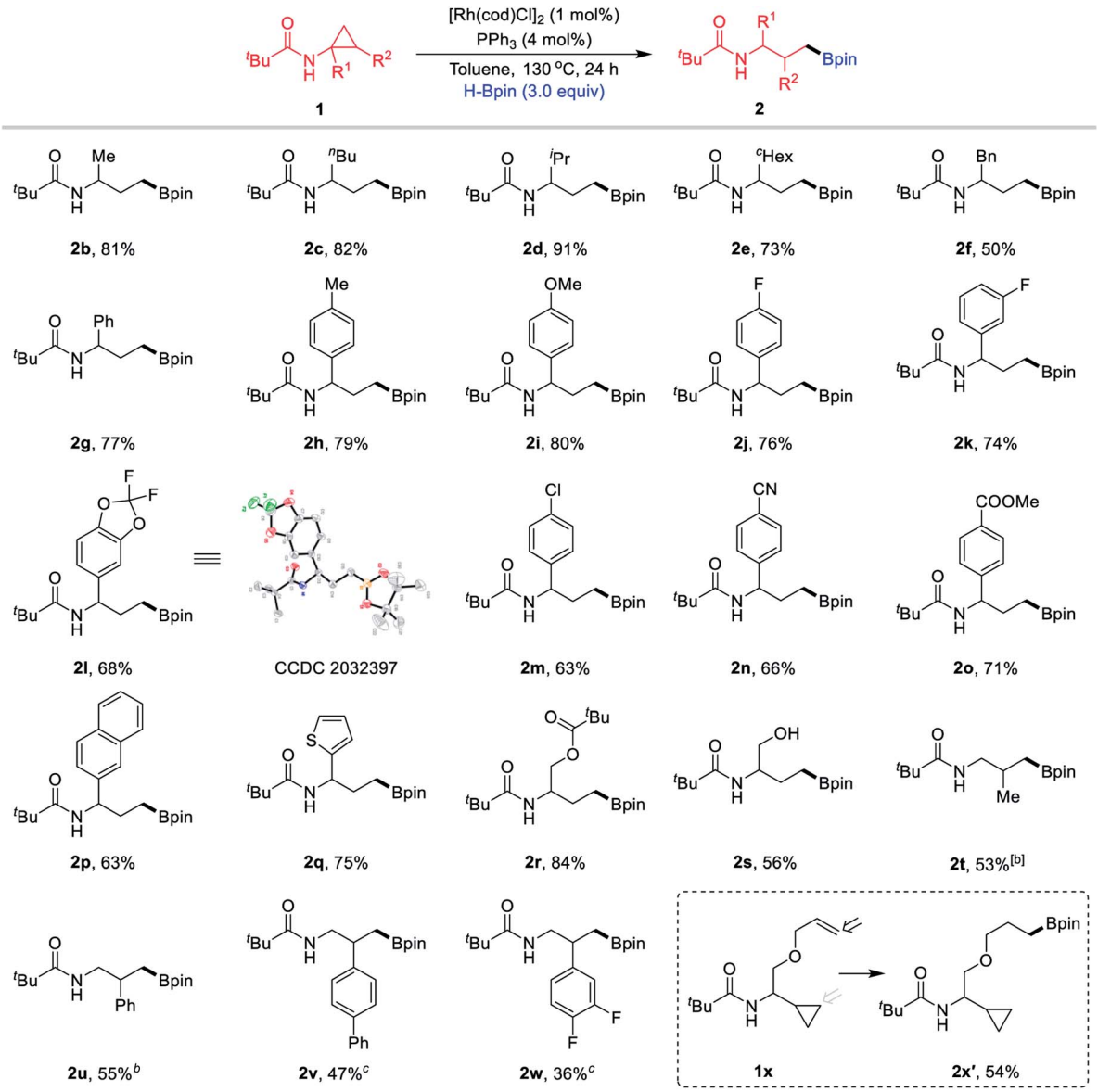

[a] Reaction conditions: $[Rh(cod)Cl]_2$ (1 mol%), PPh_3 (4 mol%), **1** (0.20 mmol), HBpin (0.6 mmol), in toluene (1.0 mL), 24 h, 130 °C, under argon, in sealed Schlenk tubes, yield of purified compounds after chromatography. [b] Using $[Rh(cod)Cl]_2$ (2.5 mol%), PPh_3 (10 mol%), 36 h, 130 °C. [c] Using $[Rh(cod)Cl]_2$ (2.5 mol%), PPh_3 (10 mol%), 36 h, 150 °C.

Open Access Article. Published on 15 January 2021. Downloaded on 11/26/2025 5:09:30 PM.
This article is licensed under a Creative Commons Attribution-NonCommercial 3.0 Unported Licence.

(entry 12) or ligand loading to 2 mol% still resulted in good yields (entry 13). Finally, control experiments showed that PPh_3 was required for high reactivity and the inhibition of side reactions (entry 14), and no product was observed in the absence of a Rh catalyst (entry 15).

We next evaluated the influence of the steric hindrance of substituents on directing groups (Scheme 1). Changing the directing group to *N*-Ac (**4a**) displayed no reactivity for ring-opening. The directing group bearing a methylcyclohexane motif (**4b**) afforded the corresponding product **5b** in 73% yield. When a sample of **4c** containing a sterically hindered *N*-Ad moiety was subjected to the reaction conditions, the desired product **5c** was formed in a much lower yield. CPAs bearing other directing groups such as *N*-Boc (**4d**) and *N*-SO^{t}Bu (**4e**), and substrate **4f** without a directing group completely failed. These results indicate that the appropriate selection of the *N*-Piv directing group ensures high reactivity and selectivity for this transformation.

Scope of the methodology

With the optimised conditions in hand, the scope of this methodology was subsequently explored (Table 2). The alkyl chains of the amide substituent R^1, including methyl (**1b**), *n*-butyl (**1c**), isopropyl (**1d**), cyclohexyl (**1e**) and benzyl (**1f**), were converted into the corresponding boronic esters **2b–2f** in good to high yields. Phenyl (**1g**) and other aryl substituents bearing methyl (**1h**), methoxy (**1i**), fluoro (**1j–1l**), chloro (**1m**), cyano (**1n**) and ester (**1o**) were compatible at the R^1 position. Among them, product **2l** was subjected to X-ray crystallographic analysis. Beyond the use of aryl-containing CPAs, we examined naphthyl and heterocyclic substrates. Naphthyl compound **1p** was readily transformed, as was thiophene substrate **1q**. The use of the CPA **1r** with an *O*-Piv motif was also tested and the desired boronate **2r** was obtained in 84% yield. Furthermore, substrate **1s** bearing a hydroxyl group still resulted in the desired product **2s** in 56% yield. In addition, this process was not limited to substrates bearing diverse R^1 substituents, and CPAs with methyl (**1t**) and different aryl (**1u–1w**) groups at the R^2 position were also suitable starting materials to effectively afford the desired products **2t–2w** efficiently. Notably, when the substrate **1x** containing a terminal olefin motif was employed for the reaction, olefin hydroboration product **2x′** was obtained in 54% yield and the ring-opening product **2x** was not observed.

Synthetic applications

To showcase the synthetic utility of this proximal-selective hydroboration protocol, a 5.0 mmol reaction of CPA **1g** was first conducted, enabling the gram-scale synthesis of the linear product **2g** in 79% isolated yield (Scheme 2). The formed boronate group is an extremely versatile intermediate in organic synthesis, which can be converted into other functional substituents. Compound **2g** could be transformed into potassium trifluoroborate salt **4** using KHF_2 in an excellent yield. Subsequently, mild oxidation of **2g** provided the corresponding alcohol **5** in 78% yield. The Cu-catalysed Chan–Lam coupling[17] of **2g** with 4-fluorobenzamide allowed the formation of 1,3-diamide derivative **6** in 70% yield. Furthermore, Pd-catalysed Suzuki–Miyaura coupling between substrate **2g** and iodobenzene or 2-bromopyridine gave the desired products **7** and **8** efficiently.[18] The Zweifel olefination of **2g** with vinylmagnesium bromide furnished the terminal alkene product **9**.[19] In addition, the Ag-catalysed fluorination of **2g** with Selectfluor® could give the monofluoroalkane **10** in a good yield based on a protocol developed by Li and co-workers.[20]

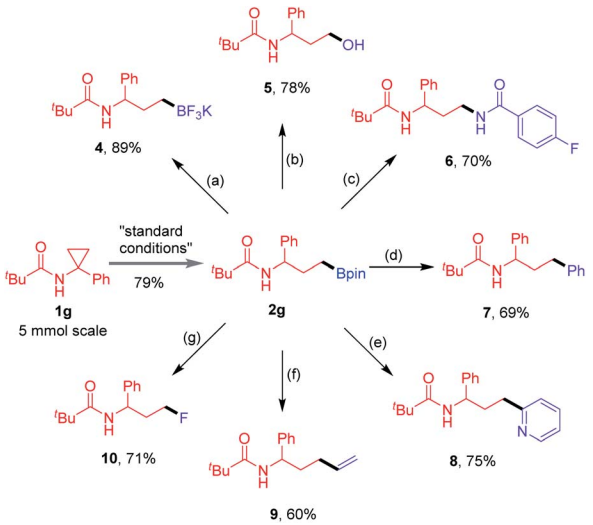

Scheme 2 Gram-scale synthesis and the follow-up transformation of compound **2g**. Reagents and conditions: (a) aq. KHF_2, MeOH, 3 h, rt; (b) $NaBO_3 \cdot 4H_2O$ (4.0 equiv.), H_2O/THF, 6 h, rt; (c) 4-fluorobenzamide (1.0 equiv.), $Cu(OAc)_2$ (10 mol%), 1,10-phen (10 mol%), $NaOSiMe_3$ (1.1 equiv.), DTBP (3.0 equiv.), 4 Å MS, ^{t}BuOH, 24 h, 75 °C; (d) PhI (1.5 equiv.), $PdCl_2(dppf) \cdot CH_2Cl_2$ (8 mol%), Ag_2O (1.5 equiv.), K_2CO_3 (3.0 equiv.), H_2O/THF, 33 h, 80 °C to rt; (e) 2-bromopyridine (1.0 equiv.), $Pd(OAc)_2$ (4 mol%), Ad_2P^nBu (12 mol%), LiO^tBu (6.0 equiv.), H_2O/THF, 24 h, 100 °C; (f) C_2H_3MgBr (6.0 equiv.), 0 °C to rt, 1 h; then I_2 (6.0 equiv.) in MeOH, −78 °C, 30 min; then NaOMe (6.0 equiv.) in MeOH, −78 °C to rt, 1.5 h; (g) $AgNO_3$ (20 mol%), Selectfluor® (3.0 equiv.), TFA (4.0 equiv.), H_2O/DCM, 5 h, 50 °C.

Mechanistic studies

Based upon the above results and the reported studies, we proposed that the transformation proceeds through four possible pathways (Fig. 2). The Rh-catalysed C–H borylation proceeds first,[16] followed by C–C activation and hydrogenation (pathway **I**). The Rh-catalysed C–C activation and β-H elimination generate an allylic amide, which further undergoes hydroboration (pathway **II**).[21] Oxidative addition of Rh species to CPAs and β-H elimination generate an enamide, and subsequently olefin migration and hydroboration (pathway **III**) take place.[22] The Rh-catalysed C–C activation and hydroboration deliver the final products directly (pathway **IV**).

Several plausible intermediates were then investigated to provide insight about the potential mechanism of this transformation (Scheme 3). The C–H borylation product **11** failed to afford the desired product **2a**, excluding pathway **I** (Scheme 3A-1). The reaction between pre-generated *N*-allylpivalamide (**12**) and HBpin could produce hydroboration product **2a** in

 © 2021 The Author(s). Published by the Royal Society of Chemistry

Open Access Article. Published on 15 January 2021. Downloaded on 11/26/2025 5:09:30 PM.
This article is licensed under a Creative Commons Attribution-NonCommercial 3.0 Unported Licence.

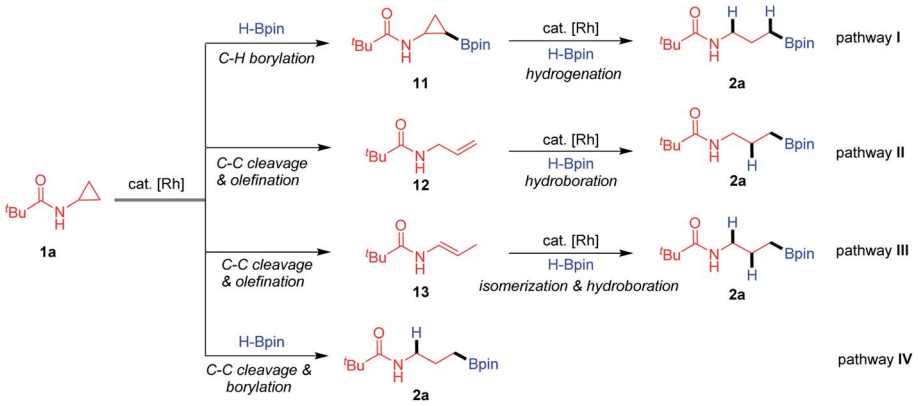

Fig. 2 Possible pathways for hydroboration of CPAs.

a modest yield (Scheme 3A-2). Impressively, treatment of substrate **1a** in the system without the addition of HBpin was found to be applicable to the formation of enamide **13** through Rh oxidative addition to the hindered proximal C–C bond (Scheme 3A-3). Moreover, this compound **13** can convert into the corresponding product **2a** by olefin isomerization and hydroboration (Scheme 3A-4). To further understand how these proximal-selective products formed, we investigated the reaction using the enantioenriched CPAs (Scheme 3B). The enantiomers (1*S*,2*R*)-**1u** (>99% ee) and (1*R*,2*S*)-**1u** (>99% ee) were, respectively, treated with HBpin under the standard conditions, giving the desired products (*R*)-**2u** and (*S*)-**2u** without erosion of the enantioselectivities. These results clearly excluded the insertion of Rh–H species onto the olefin intermediates through pathways **II** and **III**, suggesting that pathway **IV** involving direct C–C cleavage and hydroboration is possible. In order to support this proposal, we tried to isolate and characterize the key metallacyclic intermediate *via* Rh-mediated C–C bond activation of CPAs (Scheme 3C). Treatment of several CPAs with $[Rh(cod)Cl]_2$ failed to provide any stable intermediate, but fortunately, heating CPA **14** with stoichiometric $[Rh(CO)_2Cl]_2$ under neat conditions could successfully generate a dimeric rhodacyclopentanone **15**.[23] When characterized by X-ray diffraction, the Rh(I) centre in the structure of complex **15** shows axial chelation

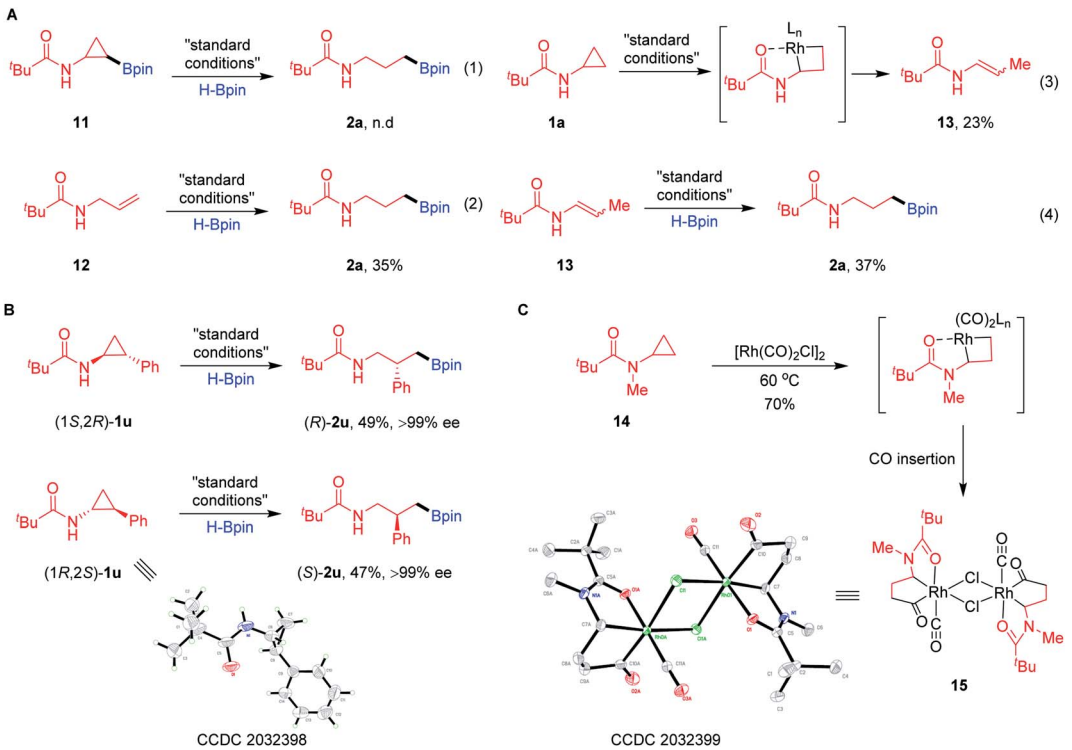

Scheme 3 Mechanistic experiments. (A) Investigation of the plausible intermediates. (B) Hydroboration of enantioenriched CPAs. (C) Synthesis of rhodacyclo complex **15**.

Open Access Article. Published on 15 January 2021. Downloaded on 11/26/2025 5:09:30 PM.
This article is licensed under a Creative Commons Attribution-NonCommercial 3.0 Unported Licence.

assisted by the *N*-Piv directing group, leading to proximal selective C–C bond cleavage and CO insertion. This establishes that Rh(I) salts are effective for insertion into the proximal C–C bond of CPAs without the assistance of HBpin.

We also performed a series of density functional theory (DFT) calculations to obtain further mechanistic information of this transformation (for computational details, see the ESI†). Fig. 3 shows the Gibbs free energy profile of this reaction. The catalytic cycle begins with a ligand exchange that replaces a cod ligand in the stable intermediate **A** with substrate **1a**. Directed by the amide oxygen, a subsequent proximal C–C bond cleavage of **1a** takes place which affords **C**. This is the rate-limiting step in the catalytic cycle ($\Delta G^{\neq} = 35.5$ kcal mol^{-1}). In this C–C bond cleavage step, we found that the non-directed transition states for both proximal and distal cleavage are unfavourable (for details, see the ESI†). Then we computed two possible pathways for hydroboration of **C**, oxidative addition and σ-complex assisted metathesis (σ-CAM).[24] It was found that H–B oxidative addition to form Rh(V) species **K** is endergonic by 39.5 kcal mol^{-1}. Alternatively, the σ-CAM pathway is much more favourable. The free energy of the four-membered cyclic σ-CAM transition state **TS2** for the formation of intermediate **D** from intermediate **C** and Hbpin is 23.7 kcal mol^{-1}. We also calculated other possible σ-CAM transition states (**TS7**–**TS9**), which would afford other hydroboration products, and found them to be higher in energy. From **D**, the re-coordination of the cod ligand leads to **E**, which reductively eliminates the C–H bond and forms the product-coordinated **F**. We also located a side pathway that corresponds to the formation of alkene products. From **C**, the directing group may dissociate from the metal centre to form intermediate **G**. Then, a β-H elimination (**TS4**) takes place which forms π-allyl–Rh(III) complex **H**. The C–H bond subsequently undergoes reductive elimination *via* **TS5** or **TS6** to produce **I** or **J**, respectively. The enamide **I** is the kinetically favoured product, and its negative free energy (−2.1 kcal mol^{-1}) supports the observation of **13** in Scheme 3A-

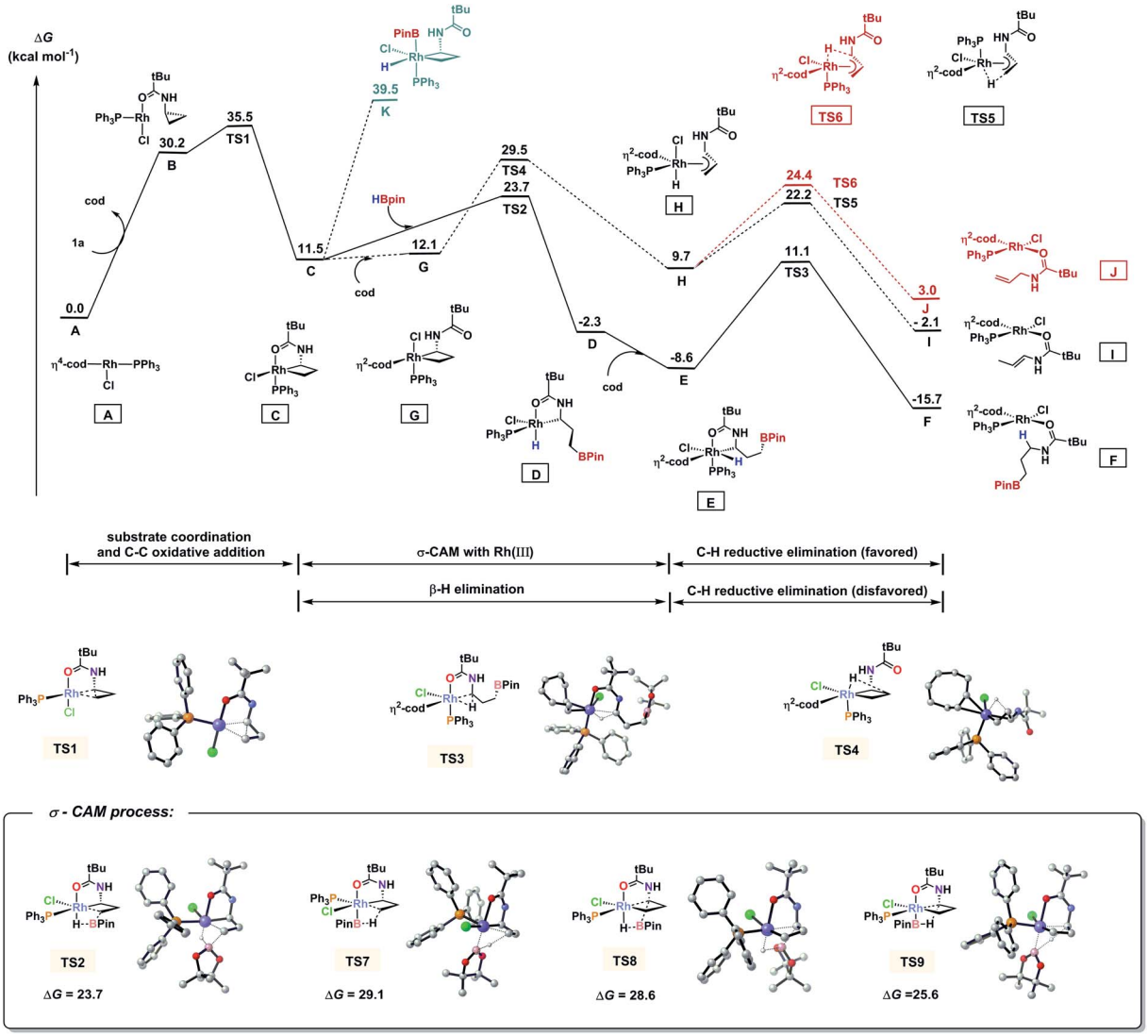

Fig. 3 Free energy diagram of hydroboration of CPAs using PPh_3 as the ligand and DFT-computed four transition states for the σ-CAM pathways. Energies are in kcal mol^{-1}.

 © 2021 The Author(s). Published by the Royal Society of Chemistry

Open Access Article. Published on 15 January 2021. Downloaded on 11/26/2025 5:09:30 PM.
This article is licensed under a Creative Commons Attribution-NonCommercial 3.0 Unported Licence.

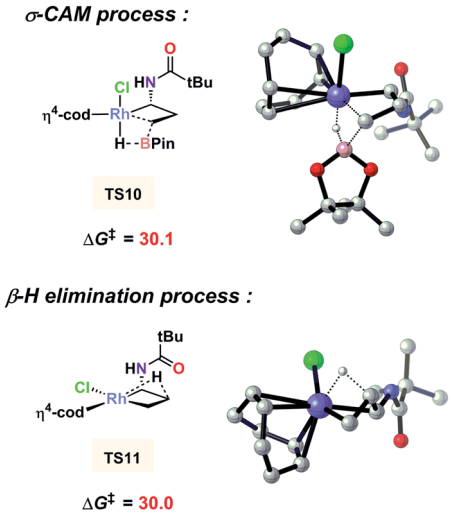

Fig. 4 DFT-computed free energies for the two competitive pathways without PPh_3 as the ligand. The zero point is $[Rh(cod)Cl]_2$. Energies are in kcal mol^{-1}.

3, where HBpin is not added. This also indicated that, under standard conditions, alkene **12** and **13** can be reversely converted into **C** (for **12**, from **J** *via* **TS6** and **TS4** with a barrier of 26.5 kcal mol^{-1}; for **13**, from **I** *via* **TS5** and **TS4** with a barrier of 31.6 kcal mol^{-1}), and then they enter the hydroboration catalytic cycle to afford **2a**, as observed in Scheme 3A-3 and A-4.

It is noted that ligand PPh_3 plays an important role in regulating the competition of σ-CAM and β-H elimination from the C–C bond cleavaged intermediate. As shown in Fig. 3, the free energy of the β-H elimination pathway *via* **TS4** is 5.8 kcal mol^{-1} higher than that of the σ-CAM process through **TS2** (29.5 *versus* 23.7 kcal mol^{-1}). However, in the absence of PPh_3, the β-H elimination transition state **TS11** is even 0.1 kcal mol^{-1} lower in energy than the corresponding σ-CAM transition state **TS10** (30.0 *versus* 30.1 kcal mol^{-1}, Fig. 4). As a result, the efficiency of the desired hydroboration was very poor with many side reactions (Table 1, entry 14). These results imply that the electron-rich nature of the PPh_3 ligand facilitates the σ-CAM process, inhibiting the formation of alkene byproducts.

Finally, we investigated the opposite regioselectivity of hydroboration of CPAs in two Ir catalytic systems (Table 1, entries 1 and 2). Previous computations by Yamaguchi and Yokogawa showed that the real catalyst is Ir(III) species when $[Ir(cod)OMe]_2$ and ligand ^{t}Bu-Quinox are employed.[16] As shown in Fig. 5A, our calculations indicate that the free energy of ring-opening transition state **TS12** at the distal C–C bond is 2.2 kcal mol^{-1} lower than that of **TS13** at the proximal C–C bond. However, the hydroboration of CPAs using $[Ir(cod)Cl]_2$ and PPh_3 involves Ir(I) species as the catalyst (Fig. 5B). The free energy of **TS15** with proximal selectivity is 4.1 kcal mol^{-1} lower than that of **TS14** with distal selectivity. These computational results are in good agreement with the observed selectivities in experiments. We also applied the distortion/interaction analysis on these transition states to understand the origins of the regioselectivity.[25] In the Ir(III) system, the distortion, particularly

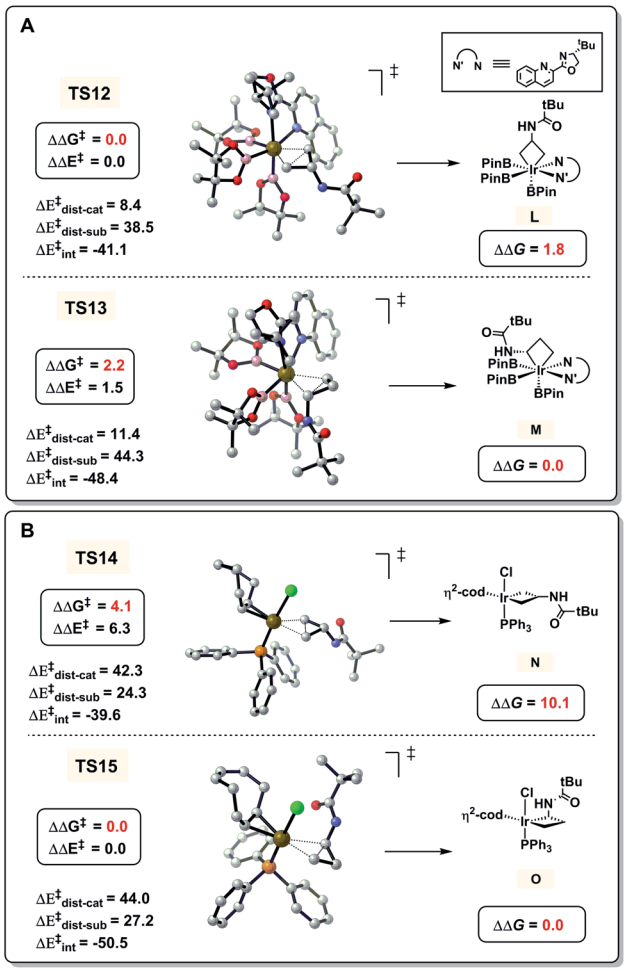

Fig. 5 DFT-computed energies and distortion/interaction analysis of C–C activation transition states. (**A**) $[Ir(cod)OMe]_2$ and ^{t}Bu-Quinox as ligands. (**B**) $[Ir(cod)Cl]_2$ and PPh_3 as ligands. Energies are in kcal mol^{-1}.

the distortion of the catalyst, controls the regioselectivity. To activate the sterically more hindered proximal C–C bond *via* **TS13**, the trigonal bipyramidal Ir(III) catalyst requires a distortion energy of 11.4 kcal mol^{-1}, which is 3.0 kcal mol^{-1} higher than that in **TS12** to break the less hindered distal C–C bond (11.4 *versus* 8.4 kcal mol^{-1}, Fig. 5A), leading to the distal-selectivity. By contrast, the favorable interaction between **1a** and the catalyst determines the regioselectivity in the Ir(I) system (Fig. 5B), which favors proximal-selective C–C bond activation significantly (−50.5 kcal mol^{-1} for **TS15** *versus* −39.6 kcal mol^{-1} for **TS14**). The tetrahedral structure of the Ir(I) catalyst makes the Ir center sterically less crowded compared with the trigonal bipyramidal Ir(III) catalyst. This favors the formation of the thermodynamically more stable intermediate **O** (*versus* **N**) with proximal-selectivity in the Ir(I) system, while less stable intermediate **L** (*versus* **M**) with distal-selectivity is preferred in the case of the Ir(III) catalyst.

Conclusions

In summary, we developed the first proximal-selective C–C bond activation followed by hydroboration of CPAs with HBpin

Open Access Article. Published on 15 January 2021. Downloaded on 11/26/2025 5:09:30 PM.
This article is licensed under a Creative Commons Attribution-NonCommercial 3.0 Unported Licence.

leading to interesting γ-amino boronates enabled by the rhodium catalyst. The key to the high chemoselectivity and regioselectivity is the selection of PPh_3 as the ligand. Significantly, experimental and computational mechanistic studies greatly provided insight into the reactivity and selectivity of this transformation. Further investigations of enantioselective variants and different types of C–C functionalizations of CPAs with tunable distal and proximal selectivity are currently underway in our laboratory.

Conflicts of interest

There are no conflicts to declare.

Acknowledgements

We would like to thank the National Natural Science Foundation of China (Grant 21672097, 21972064, and 21803030), the Fundamental Research Funds for the Central Universities, the National Natural Science Foundation of Jiangsu Province (Grant BK20170632 and BK20170631), the Excellent Youth Foundation of Jiangsu Scientific Committee (Grant BK20180007), and the "Innovation & Entrepreneurship Talents Plan" of Jiangsu Province for their financial support.

Notes and references

1 (*a*) I. A. I. Mkhalid, J. H. Barnard, T. B. Marder, J. M. Murphy and J. F. Hartwig, *Chem. Rev.*, 2010, **110**, 890; (*b*) J. F. Hartwig, *Chem. Soc. Rev.*, 2011, **40**, 1992; (*c*) J. F. Hartwig, *Acc. Chem. Res.*, 2012, **45**, 864; (*d*) A. Ros, R. Fernández and J. M. Lassaletta, *Chem. Soc. Rev.*, 2014, **43**, 3229; (*e*) W. L. A. Brooks and B. S. Sumerlin, *Chem. Rev.*, 2016, **116**, 1375; (*f*) E. C. Neeve, S. J. Geier, I. A. I. Mkhalid, S. A. Westcott and T. B. Marder, *Chem. Rev.*, 2016, **116**, 9091; (*g*) A. B. Cuenca, R. Shishido, H. Ito and E. Fernández, *Chem. Soc. Rev.*, 2017, **46**, 415; (*h*) J. W. B. Fyfe and A. J. B. Watson, *Chem*, 2017, **3**, 31; (*i*) B. S. L. Collins, C. M. Wilson, E. L. Myers and V. K. Aggarwal, *Angew. Chem., Int. Ed.*, 2017, **56**, 11700; (*j*) M. Wang and Z. Shi, *Chem. Rev.*, 2020, **120**, 7348.

2 (*a*) K. M. Logan, K. B. Smith and M. K. Brown, *Angew. Chem., Int. Ed.*, 2015, **54**, 5228; (*b*) L. Zhang, G. J. Lovinger, E. K. Edelstein, A. A. Szymaniak, M. P. Chierchia and J. P. Morken, *Science*, 2016, **351**, 70; (*c*) J. Hu, Y. Zhao, J. Liu, Y. Zhang and Z. Shi, *Angew. Chem., Int. Ed.*, 2016, **55**, 8718; (*d*) Y. Huang, K. B. Smith and M. K. Brown, *Angew. Chem., Int. Ed.*, 2017, **56**, 13314; (*e*) M. Kischkewitz, K. Okamoto, C. Mück-Lichtenfeld and A. Studer, *Science*, 2017, **355**, 936; (*f*) L. Wang, T. Zhang, W. Sun, Z. He, C. Xia, Y. Lan and C. Liu, *J. Am. Chem. Soc.*, 2017, **139**, 5257; (*g*) K. M. Logan, S. R. Sardini, S. D. White and M. K. Brown, *J. Am. Chem. Soc.*, 2018, **140**, 159; (*h*) Z. Liu, H. Ni, T. Zeng and K. M. Engle, *J. Am. Chem. Soc.*, 2018, **140**, 3223; (*i*) Y. Cheng, C. Mück-Lichtenfeld and A. Studer, *J. Am. Chem. Soc.*, 2018, **140**, 6221; (*j*) R. Kojima, S. Akiyama and H. Ito, *Angew. Chem., Int. Ed.*, 2018, **57**, 7196; (*k*) P. Gao, C. Yuan, Y. Zhao and Z. Shi, *Chem*, 2018, **4**, 2201; (*l*) J. Hu, Y. Zhao and Z. Shi, *Nat. Catal.*, 2018, **1**, 860; (*m*) J. A. Myhill, C. A. Wilhelmsen, L. Zhang and J. P. Morken, *J. Am. Chem. Soc.*, 2018, **140**, 15181; (*n*) J. Li, H. Wang, Z. Qiu, C.-Y. Huang and C.-J. Li, *J. Am. Chem. Soc.*, 2020, **142**, 13011; (*o*) M. R. Jones, C. D. Fast and N. D. Schley, *J. Am. Chem. Soc.*, 2020, **142**, 6488; (*p*) R. Oeschger, B. Su, I. Yu, C. Ehinger, E. Romero, S. He and J. Hartwig, *Science*, 2020, **368**, 736; (*q*) L. Wang, T. Zhao, W. Sun, Z. He, C. Xia, Y. Lan and C. liu, *J. Am. Chem. Soc.*, 2017, **139**, 5257; (*r*) Y. Hu, W. Sun, T. Zhang, N. Xu, Y. Lan and C. Liu, *Angew. Chem., Int. Ed.*, 2019, **58**, 15813; (*s*) C. Law, E. Kativhu, J. Wang and J. P. Morken, *Angew. Chem., Int. Ed.*, 2020, **59**, 10311; (*t*) S. Namirembe and J. P. Morken, *Chem. Soc. Rev.*, 2019, **48**, 3464; (*u*) D. Ni, B. P. Witherspoon, H. Zhang, C. Zhou, K. N. Houk and M. K. Brown, *Angew. Chem., Int. Ed.*, 2020, **59**, 11432; (*v*) D. Wang, C. Mück-Lichtenfeld and A. Studer, *J. Am. Chem. Soc.*, 2020, **142**, 9119; (*w*) C. You and A. Studer, *Angew. Chem., Int. Ed.*, 2020, **59**, 17245.

3 L. A. William and B. S. Sumerlin, *Chem. Rev.*, 2016, **116**, 1375.

4 (*a*) P. C. Trippier and C. McGuigan, *MedChemComm*, 2010, **1**, 183; (*b*) H. S. ban and H. Nakamura, *Chem. Rec.*, 2015, **15**, 616; (*c*) L. K. H. Leung, T. Brown Jr, C. J. Schofield and T. W. Claridge, *MedChemComm*, 2011, **2**, 390; (*d*) K. M. E. Tehrani and N. Martin, *MedChemComm*, 2018, **9**, 1439; (*e*) J. P. M. Antonio, R. Russo, C. P. Carvalho, P. M. S. D. Cal and P. M. P. Gois, *Chem. Soc. Rev.*, 2019, **48**, 3513.

5 (*a*) H. Brown and B. C. Rao, *J. Org. Chem.*, 1957, **22**, 1137; (*b*) D. Wang, X.-S. Xue, K. N. Houk and Z. Shi, *Angew. Chem., Int. Ed.*, 2018, **57**, 16861.

6 (*a*) J. D. Hewes, C. W. Kreimendahl, T. B. Marder and M. F. Hawthorne, *J. Am. Chem. Soc.*, 1984, **106**, 5757; (*b*) D. Männig and H. Nöth, *Angew. Chem., Int. Ed.*, 1985, **24**, 878; (*c*) K. Burgess, W. A. van der Donk, S. A. Westcott, T. B. Marder, R. T. Baker and J. C. Calabrese, *J. Am. Chem. Soc.*, 1992, **114**, 9350; (*d*) A. H. Hoveyda, D. A. Evans and G. C. Fu, *Chem. Rev.*, 1993, **93**, 1307; (*e*) K. Burgess and M. J. Ohlmeyer, *Chem. Rev.*, 1991, **91**, 1179; (*f*) C. M. Crudden and D. Edwards, *Eur. J. Org. Chem.*, 2003, **24**, 4695; (*g*) C. A. Vogels and S. A. Westcott, *Curr. Org. Chem.*, 2005, **9**, 687.

7 (*a*) G. Wang, X. Liang, L. Chen, Q. Gao, J.-G. Wang, P. Zhang, Q. Peng and S. Xu, *Angew. Chem., Int. Ed.*, 2019, **58**, 8187; (*b*) X.-Y. Bai, W. Zhao, X. Sun and B.-J. Li, *J. Am. Chem. Soc.*, 2019, **141**, 19870.

8 (*a*) D. A. Evans and G. C. Fu, *J. Am. Chem. Soc.*, 1991, **113**, 4042; (*b*) S. M. Smith and J. M. Takacs, *J. Am. Chem. Soc.*, 2010, **132**, 1740; (*c*) S. M. Smith, N. C. Thacker and J. M. Takacs, *J. Am. Chem. Soc.*, 2008, **130**, 3734; (*d*) V. M. Shoba, N. C. Thacker, A. J. Bochat and J. M. Takacs, *Angew. Chem., Int. Ed.*, 2016, **55**, 1465; (*e*) S. Chakrabarty and J. M. Takacs, *J. Am. Chem. Soc.*, 2017, **139**, 6066; (*f*) Y. Xi and J. F. Hartwig, *J. Am. Chem. Soc.*, 2016, **138**, 6703; (*g*) G. L. Hoang and J. M. Takacs, *Chem. Sci.*, 2017, **8**, 4511;

 © 2021 The Author(s). Published by the Royal Society of Chemistry

Open Access Article. Published on 15 January 2021. Downloaded on 11/26/2025 5:09:30 PM.
This article is licensed under a Creative Commons Attribution-NonCommercial 3.0 Unported Licence.

(*h*) H. Zhao, Q. Gao, Y. Zhang, P. Zhang and S. Xu, *Org. Lett.*, 2020, **22**, 2861.

9 (*a*) R. L. Reyes, T. Iwai, S. Maeda and M. Sawamura, *J. Am. Chem. Soc.*, 2019, **138**, 6817; (*b*) Y. Shi, Q. Gao and S. Xu, *J. Am. Chem. Soc.*, 2019, **141**, 10599; (*c*) R. L. Reyes, M. Sato, T. Iwai and M. Sawamura, *J. Am. Chem. Soc.*, 2020, **139**, 589; (*d*) L. Chen, Y. Yang, L. Liu, Q. Gao and S. Xu, *J. Am. Chem. Soc.*, 2020, **142**, 12062.

10 R. L. Reyes, M. Sato, T. Iwai, K. Suzuki, S. Maeda and M. Sawamura, *Science*, 2020, **369**, 970.

11 (*a*) H. Lebel, J.-F. Marcoux, C. Molinaro and A. B. Charette, *Chem. Rev.*, 2003, **103**, 977; (*b*) A. Reichelt and S. F. Martin, *Acc. Chem. Res.*, 2006, **39**, 433; (*c*) D. Y.-K. Chen, R. H. Pouwer and J.-A. Richard, *Chem. Soc. Rev.*, 2012, **41**, 4631; (*d*) C. Ebner and E. M. Carreira, *Chem. Rev.*, 2017, **117**, 11651.

12 (*a*) O. O. Sokolova and J. F. Bower, *Chem. Rev.*, 2021, **121**, 80; (*b*) V. Pirenne, B. Muriel and J. Waser, *Chem. Rev.*, 2021, **121**, 227.

13 S. Miyamura, M. Araki, T. Suzuki, J. Yamaguchi and K. Itami, *Angew. Chem., Int. Ed.*, 2015, **54**, 846.

14 (*a*) F. Chen, T. Wang and N. Jiao, *Chem. Rev.*, 2014, **114**, 8613; (*b*) L. Souillart and N. Cramer, *Chem. Rev.*, 2015, **115**, 9410; (*c*) D.-S. Kim, W.-J. Park and C.-H. Jun, *Chem. Rev.*, 2017, **117**, 8977; (*d*) G. Fumagalli, S. Stanton and J. F. Bower, *Chem. Rev.*, 2017, **117**, 9404; (*e*) F. Song, T. Gou, B.-Q. Wang and Z.-J. Shi, *Chem. Soc. Rev.*, 2018, **47**, 7078; (*f*) H. Lu, T.-Y. Yu, P.-F. Xu and H. Wei, *Chem. Rev.*, 2021, **121**, 365; (*g*) M. Murakami and N. Ishida, *Chem. Rev.*, 2021, **121**, 264; (*h*) Y. Xia and G. Dong, *Nat. Rev. Chem.*, 2020, **4**, 600.

15 (*a*) C. Li, J. Wang, L. M. Barton, S. Yu, M. Tian, D. S. Peters, M. Kumar, A. W. Yu, K. A. Johnson, A. K. Chatterjee, M. Yan and P. S. Baran, *Science*, 2017, **356**, eaam7355; (*b*) A. Fawcett, J. Pradeilles, Y. Wang, T. Mutsuga, E. L. Myers and V. K. Aggarwal, *Science*, 2017, **357**, 283; (*c*) A. Noble, R. S. Mega, D. Pflästerer, E. L. Myers and V. K. Aggarwal, *Angew. Chem., Int. Ed.*, 2018, **57**, 2155.

16 H. Kondo, S. Miyamura, K. Matsushita, H. Kato, C. Kobayashi, Arifin, K. Itami, D. Yokogawa and J. Yamaguchi, *J. Am. Chem. Soc.*, 2020, **142**, 11306.

17 J.-Q. Chen, J.-H. Li and Z.-B. Dong, *Adv. Synth. Catal.*, 2020, **362**, 3311.

18 C.-T. Yang, Z.-Q. Zhang, H. Tajuddin, C.-C. Wu, J. Liang, J.-H. Liu, Y. Fu, M. Czyzewska, P. G. Steel, T. B. Marder and L. Liu, *Angew. Chem., Int. Ed.*, 2012, **51**, 528.

19 R. J. Armstrong and V. K. Aggarwal, *Synthesis*, 2017, **49**, 3323.

20 Z. Li, Z. Wang, L. Zhu, X. Tan and C. Li, *J. Am. Chem. Soc.*, 2014, **136**, 16439.

21 (*a*) N. G. McCreanor, S. Stanton and J. F. Bower, *J. Am. Chem. Soc.*, 2016, **138**, 11465; (*b*) H. Kondo, K. Itami and J. Yamaguchi, *Chem. Sci.*, 2017, **8**, 3799.

22 (*a*) C. Romano, D. Fiorito and C. Mazet, *J. Am. Chem. Soc.*, 2019, **141**, 16983; (*b*) X. Chen, Z. Cheng, J. Guo and Z. Lu, *Nat. Commun.*, 2018, **9**, 3939.

23 (*a*) M. H. Shaw, E. Y. Melikhova, D. P. Kloer, W. G. Whittingham and J. F. Bower, *J. Am. Chem. Soc.*, 2013, **135**, 4992; (*b*) M. H. Shaw, N. G. McCreanor, W. G. Whittingham and J. F. Bower, *J. Am. Chem. Soc.*, 2015, **137**, 463; (*c*) G.-W. Wang and J. F. Bower, *J. Am. Chem. Soc.*, 2018, **140**, 2743.

24 R. N. Perutz and S. Sabo-Etienne, *Angew. Chem., Int. Ed.*, 2007, **46**, 2578.

25 F. M. Bickelhaupt and K. N. Houk, *Angew. Chem., Int. Ed.*, 2017, **56**, 10070.

© 2021 The Author(s). Published by the Royal Society of Chemistry